1952 *J. Am. Chem. Soc.* **1982**, *104*, 1952-1957

Benzoquinone Quenching of Diporphyrin Excited States: Kinetic Evidence for Distinguishing Electron-Transfer Photoproducts from (π,π*) States

T. L. Netzel,*,† M. A. Bergkamp,† and C. K. Chang‡

Contribution from the Departments of Chemistry, Brookhaven National Laboratory, Upton, New York 11973, and Michigan State University, East Lansing, Michigan 48824.

Received July 30, 1981

Abstract: Previous spectroscopic work[6] on a doubly linked cofacial diporphyrin, Mg–H$_2$(5), comprised of magnesium porphyrin and free-base porphyrin subunits provided optical evidence consonant with rapid (>10^{11} s^{-1}) light-driven electron transfer (ET) between the subunits in CH$_2$Cl$_2$ and $^1(\pi,\pi^*)$ excited state formation in tetrahydrofuran (THF). We report here that the spectral and kinetic results due to quenching the excited states of Mg–H$_2$(5) in these two solvents by the addition of iodobenzene and *p*-benzoquinone confirm the excited state assignments suggested earlier. We also propose a working model of excited state couplings for Mg–H$_2$(5) in CH$_2$Cl$_2$ to account for the rapidity (>10^{11} s^{-1}) of the forward ET reaction and the slowness (5 × 10^9 s^{-1}) of the reverse one. Finally, the rates and thermodynamic efficiencies of these in vitro ET reactions are shown to compare favorably with those of the primary charge separations found in natural photosystems.

Numerous studies of natural photosystems[1-5] (e.g., reaction centers (RC's) of photosynthetic bacteria and photosystem I (PSI) and photosystem II (PSII) of green plants) have shown that the earliest detectable chemical reactions are light-driven electron transfers. These electron transfers occur between chlorophyll or bacteriochlorophyll (BChl) electron donors and chlorophyll, pheophytin (a Mg-free chlorophyll), or bacteriopheophytin (BPheo) electron acceptors in the subnanosecond time domain. An earlier paper[6] reported optical evidence consonant with a <6 ps light-driven electron transfer between a magnesium porphyrin and a metal-free porphyrin in a doubly linked cofacial diporphyrin, Mg–H$_2$(5). The photoproduct [Mg$^{+\cdot}$–H$_2^{-\cdot}$(5)], a magnesium porphyrin cation and a free-base porphyrin anion, is stable for hundreds of picoseconds. This result contrasts sharply with those found when photoexcited porphyrins and chlorophylls are quenched under bimolecular conditions by the addition of uncharged electron acceptors (e.g., quinones or nitroaromatics).[7,8] Stable electron-transfer (ET) products (cations and anions) are detected only when the quenching reaction proceeds from a triplet excited state (T$_1$),[9] but not when the reaction proceeds from a singlet excited state (S$_1$). These results were rationalized[7,10,11] by postulating that both singlet and triplet states were quenched by the production of radical pair ET products. However, the product of singlet state quenching would be a singlet radical pair which presumably re-forms the singlet ground states of the reactants in much less time than is required for the cation and anion fragments to separate. In contrast, triplet state quenching would form a triplet radical pair. In this case the reduction of the cation by the anion is spin forbidden and evidently slow enough so that the ions can separate. The extreme rapidity of the first ETs in natural photosystems[4,5] (>10^{11} s^{-1}) demands that they proceed from singlet states. Yet the reverse ET is slow enough (~10^8 s^{-1} in photosynthetic bacteria[12]) that the quantum yield of secondary ETs is near 100%. This apparent paradox focuses attention on the molecular properties of the electron acceptor. Indeed, the available optical data on diporphyrins suggest that a detectable singlet biradical ET product can be formed if the electron acceptor is a free-base porphyrin.[6]

The initial study of the photochemistry of the Mg–H$_2$(5) diporphyrin noted that the change-in-absorbance (ΔA) spectra and kinetics in tetrahydrofuran (THF) were different from those in CH$_2$Cl$_2$. (Mg–H$_2$(5) has the same structure[13] as diporphyrin (I), labeled H$_2$–H$_2$(5), except that the central two H atoms on one porphyrin subunit have been replaced with a Mg atom; R$_1$ = *n*-octyl; R$_2$ = –CH$_2$C(=O)N(*n*-Bu)CH$_2$CH$_2$–. Mg–Mg(5) also has the same structure as I, except both porphyrin subunits have central Mg atoms.) In THF, the ΔA spectra were similar to those due to excited singlet state formation in the symmetric diporphyrins Mg–Mg(5) and H$_2$–H$_2$(5). In CH$_2$Cl$_2$, the ΔA spectra showed a strong, broad absorption feature in the 660-nm region where both magnesium porphyrin cations and free-base porphyrin anions are known to absorb.[14] These results were also consistent with electrochemical estimates[6] of the likelihood of forming ET products from the S$_1$ state of Mg–H$_2$(5) in the two solvents. In

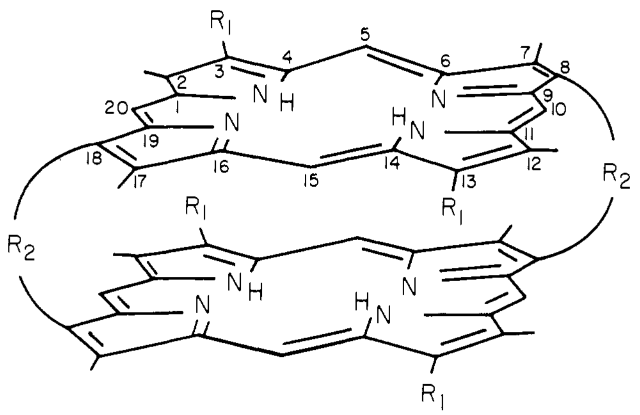

I

---

† Brookhaven National Laboratory.

‡ Michigan State University.

(1) Katz, J. J.; Norris, J. R.; Shipman, L. L.; Thurnaur, M. C.; Wasielewski, M. R. *Annu. Rev. Biophys. Bioeng.* **1978**, *7*, 393.

(2) McElroy, J. D.; Feher, G.; Mauzerall, D. C. *Biochim. Biophys. Acta* **1972**, *267*, 363.

(3) Klimov, V. V.; Klevanik, A. V.; Shuvalov, U. A.; Krasnovski, A. A. *FEBS Lett.* **1977**, *82*, 183.

(4) Kaufman, K. J.; Dutton, P. L.; Netzel, T. L.; Leigh, J. S.; Rentzepis, P. M. *Science* **1973**, *188*, 1301.

(5) Rockley, M. G.; Windsor, M. W.; Cogdell, R. J.; Parson, W. W. *Proc. Natl. Acad. Sci. U.S.A.* **1975**, *72*, 2251.

(6) Netzel, T. L.; Kroger, P.; Chang, C.-K.; Fujita, I.; Fajer, J. *Chem. Phys. Lett.* **1979**, *67*, 223.

(7) Holten, D.; Gouterman, M.; Parson, W. W.; Windsor, M. W.; Rockley, M. G. *Photochem. Photobiol.* **1976**, *23*, 415.

(8) Huppert, D.; Rentzepis, P. M.; Tollin, G. *Biochim. Biophys Acta* **1976**, *440*, 356.

(9) Harriman, A.; Porter, G.; Searle, N. *J. Chem. Soc., Faraday Trans. 2* **1979**, *75*, 1514.

(10) Gouterman, M.; Holten, D. *Photochem. Photobiol.* **1977**, *25*, 85.

(11) Seely, G. R. *Photochem. Photobiol.* **1978**, *27*, 639.

(12) Parson, W. W.; Clayton, R. K.; Cogdell, R. J. *Biochim. Biophys. Acta* **1975**, *387*, 265.

(13) Chang, C.-K. *J. Heterocycl. Chem.* **1977**, *14*, 1285.

(14) Fujita, I.; Fajer, J., private communication.

0002-7863/82/1504-1952$01.25/0

THF such a reaction was endergonic by 0.080 eV, while in CH_2Cl_2 it was exergonic by 0.150 eV. If the above interpretation of $^1(\pi,\pi^*)$ formation in THF and ET product, $Mg^{+\cdot}–H_2^{-\cdot}(5)$, formation in CH_2Cl_2 is correct, it is reasonable to expect these states to have different physical and chemical properties.

Here we report the effects of perturbing these excited states by the addition of a heavy-atom solvent (iodobenzene) and quenching them with *p*-benzoquinone (BQ). In addition a quantitative comparison of their ΔA spectra is provided along with a kinetic analysis of their lifetimes. The results confirm the assignments suggested earlier[6] and justify describing a working model of the forward and reverse ET processes for $Mg–H_2(5)$ in CH_2Cl_2.

Experimental Procedures

The Nd-glass laser apparatus described previously[15] was improved to more accurately measure change-in-absorbance (ΔA) spectra. The most significant improvement concerned the relative cross-sections of the photolysis and probe pulses. In the past a ground glass plate was used to diffuse the white probe pulse, but it was difficult to image this light to a spot much smaller than the photolysis cross-section (~1.5 mm in diameter). More accurate ΔA spectra could be produced if the probe light could be made ~0.4 mm in diameter. To this end, the glass diffuser was masked so only a 1 mm diameter spot was illuminated. Next a 0.15 m focal length lens formed an enlarged image of this spot 0.68 m from the diffuser. A second 1 mm diameter aperature reduced the size of this image which was relayed 2.5 m to the sample via a 0.5 m focal length lens positioned 0.67 m before the sample. Although probe light was lost in the above procedure, the apparatus now had a probe pulse cross-section in the sample cell significantly smaller than that of the photolysis pulse. Other improvements included (a) automation of the data acquisition cycle (including charging and firing the laser, stirring the sample, operating the photolysis shutter, monitoring the photolysis energy, and checking the probe beam intensity) and (b) computerization of the data analysis procedure (including statistical analysis of the ratios of the intensities of the sample and reference beams).

Samples ((2.5–3) × 10^{-4} M) were held in 0.2 cm path length optical cells. The cells were flame sealed on a vacuum line after 3 freeze-pump–thaw cycles. Benzoquinone (Aldrich) was purified by vacuum sublimation. Tetrahydrofuran and CH_2Cl_2 (Aldrich Reagent Grade) were used without further purification. Iodobenzene (Aldrich) was redistilled prior to use and stored in the dark. All samples were photolyzed at 527 nm with 6 ps (fwhm) pulses of 1–2 mJ energy. Energy-dependent studies of the ΔA immediately after photolysis showed that the samples were completely photolyzed throughout this energy range.

Results

ΔA Spectra in THF and CH_2Cl_2. The ΔA spectra of $Mg–H_2(5)$ in THF/iodobenzene (1:1) and CH_2Cl_2 at 0 ps are shown in Figure 1. The differences between the two spectra are most likely due to two different electronic excited states. However, an alternative explanation, a single electronic excited state with the differences being induced by changing solvents, cannot be ruled out a priori. It is worth noting, though, that the ground state absorption spectrum of $Mg–H_2(5)$ is only mildly affected by changing the solvent. Kinetic plots of ΔA vs. time for $Mg–H_2(5)$ in neat THF and CH_2Cl_2 are given in the upper portion of Figures 2 and 3, respectively. For $Mg–H_2(5)$ in THF, the decay of the initial photoproduct (S_1) is not described by a single exponential rate. This indicates the presence of a second, longer-lived transient (presumably T_1), but lack of data beyond 5 ns prevents the determination of either the S_1 or T_1 lifetimes. However, the upper and lower limits of the lifetime of the initial state (S_1) are 1.5 and 4.0 ns (asymptote of the initial decay equal to ΔA at 5 ns [$\Delta A(t = 5\ \text{ns})$] and zero, respectively). In fact the data for $Mg–H_2(5)$ in both CH_2Cl_2 and THF are described by

$$\Delta A(t) = [\Delta A(t = 0) - \beta]e^{-(\lambda_1 t)} + \beta e^{-(\lambda_2 t)} \qquad (1)$$

where λ_1 and λ_2 are rate constants and β is the product of the quantum yield of the final long-lived state, the initial sample concentration, and the difference in molar absorbtivity between the long-lived and ground states. However in this work, β is an empirical parameter as the first and last values in this product are unknown. The best fit rate constants for the decay of photoexcited $Mg–H_2(5)$ in THF and CH_2Cl_2, as well as other solvents, are given in Table I.

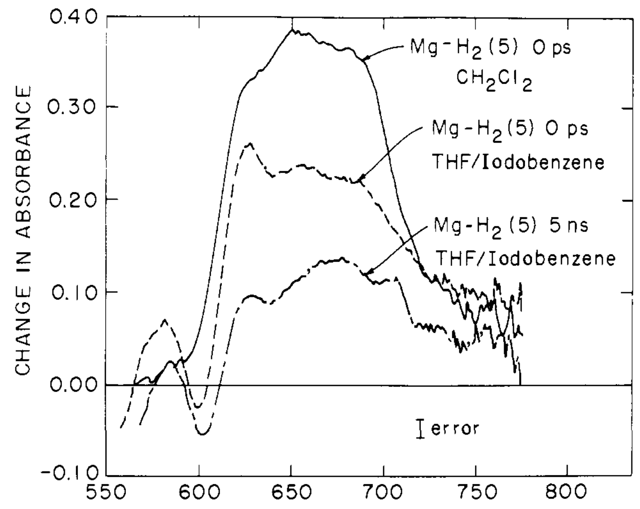

Figure 1. Change-in-absorbance (ΔA) spectra for 1.9 × 10^{-4} M $Mg–H_2(5)$: in CH_2Cl_2 immediately after excitation, *t* = 0 ps; in THF/iodobenzene (1:1), *t* = 0 ps; and in THF/iodobenzene (1:1), *t* = 5 ns.

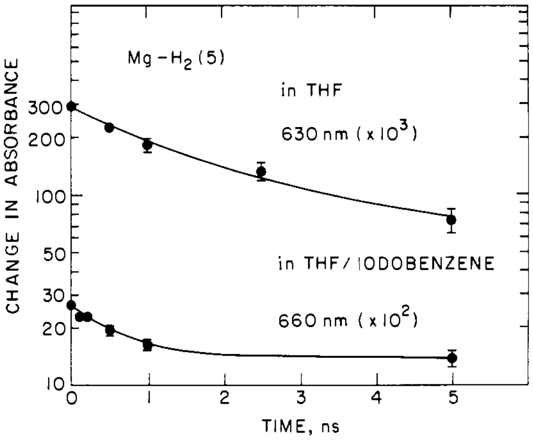

Figure 2. Kinetic plots of ΔA data for 2.2 × 10^{-4} M $Mg–H_2(5)$ in THF at 630 nm (top) and in THF/iodobenzene (1:1) at 660 nm (bottom). The solid lines are caluclated results based on eq 1 with the rate constants specified in Table I.

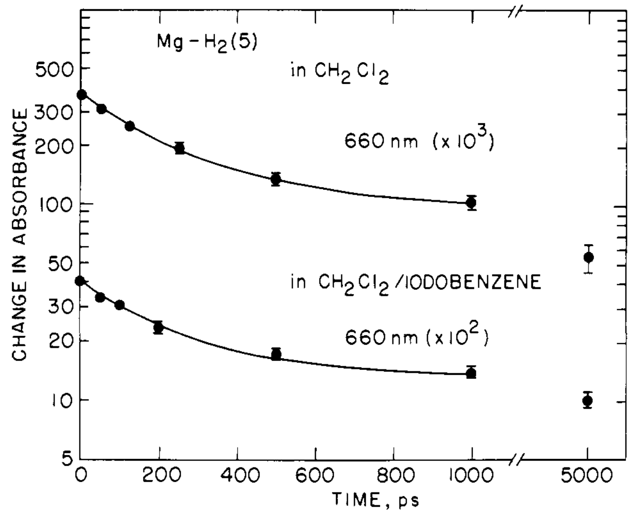

Figure 3. Kinetic plots of ΔA data for 1.9 × 10^{-4} M $Mg–H_2(5)$ in CH_2Cl_2 at 660 nm (top) and of 2.1 × 10^{-4} M $Mg–H_2(5)$ in CH_2Cl_2/iodobenzene (1:1) at 660 nm (bottom). The solid lines are calculated results based on eq 1 with the rate constants specified in Table I.

---

(15) Creutz, C.; Chou, M.; Netzel, T. L.; Okumura, M.; Sutin, N. *J. Am. Chem. Soc.* **1980**, *102*, 1309.

Table I. Mg–H_2(5) Excited State Lifetimes

solution	$\tau_1 = 1/\lambda_1$, ps	$\tau_2 = 1/\lambda_2$, ns
CH_2Cl_2	200 ± 15	$6\,(^{+3}_{-2})$
CH_2Cl_2/iodobenzene[a]	200 ± 20	$13\,(^{+6}_{-4})$
THF	~2000[b]	
THF/iodobenzene[a]	650 ± 60	>15
THF + 0.25 M BQ	25 ± 5[c]	0.47 ± 0.07
CH_2Cl_2 + 0.25 M BQ	90 ± 5	>15

[a] 1:1 by volume. [b] See the text for a discussion of the error limits. [c] The instrumental response of the laser system (due to the convolution of excitation and probe pulses) to an optical transient of <3 ps duration can be described by a Gaussian function with a fwhm of 11 ps. Equation 1 does not deconvolute this instrumental response. Thus the true τ_1 may be somewhat less than 25 ps.

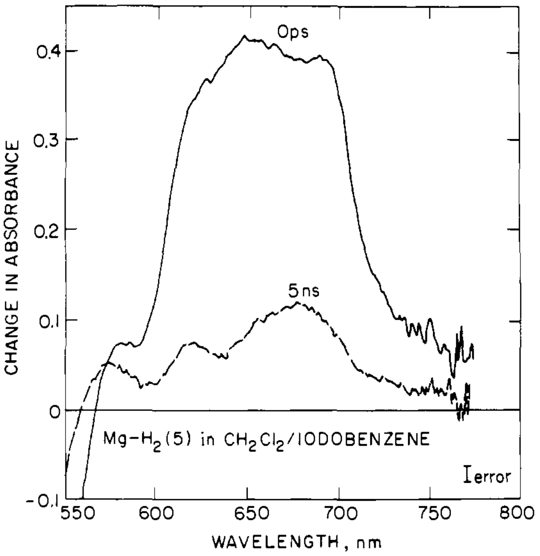

Figure 4. Change-in-absorbance spectra for 2.1 × 10^{-4} M Mg–H_2(5) in CH_2Cl_2/iodobenzene (1:1) at t = 0 ps and 5 ns.

Iodobenzene Perturbation. If the S_1 state of Mg–H_2(5) in THF [a $^1(\pi,\pi^*)$ state] is decaying to both S_0 and $^3(\pi,\pi^*)$ states, changing the solvent to THF/iodobenzene (1:1) should increase the intersystem crossing rate, $S_1 \rightarrow T_1$.[7] The kinetics for the decay of the S_1 state of Mg–H_2(5) in this solvent system are shown in the lower portion of Figure 2. In this case the decay of the initial state to a second, longer-lived state is clear and the rate constants for eq 1 which describe the data are given in Table I. The expected increase in the rate of intersystem crossing is reflected in the decreased singlet lifetime (650 ps vs. ~2 ns in neat THF). The lowest curve in Figure 1 shows the ΔA spectrum in this solvent mixture 5 ns after excitation. The $T_1 - S_0$ difference spectrum is seen to be flatter than the $S_1 - S_0$ difference spectrum shown by the middle curve of Figure 1.

A kinetic comparison of the decay of the photoproduct of Mg–H_2(5) in CH_2Cl_2 and CH_2Cl_2/iodobenzene is shown in Figure 3 and the rate constants in eq 1 which best describe the data are given in Table I. These data show that the decay of the first transient [presumably $Mg^{+\cdot}$–$H_2^{-\cdot}$(5)] is unaffected by switching from one solvent to the other. Also, the second transient decays in both solvents, but may be longer-lived in CH_2Cl_2/iodobenzene. Figure 4 shows the ΔA spectra at 0 ps and 5 ns for Mg–H_2(5) in the mixed solvent. The identity of the second transient is unclear. However, the two most likely possibilities are: one, a $^3(\pi,\pi^*)$ state of Mg–H_2(5), and two, a triplet biradical state, $^3(Mg^{+\cdot}$–$H_2^{-\cdot})$. The fact that it decays more rapidly than the T_1 state of Mg–H_2(5) found in THF/iodobenzene suggests that it is not a $^3(\pi,\pi^*)$ state. Comparison of the lowest curve in Figure 1 (T_1) and the 5 ns curve in Figure 4 also suggests that they are different states. To account for differences between the ground state absorption spectra in the two solvents, we numerically added various amounts of the corresponding ground state spectra (simulating different quantum yields of the second transient) to these ΔA curves. No choice of quantum yields could make the resulting transient absorbance spectra for these two long-lived transients agree. Although the above results are consistent with the suggestion that the long-lived transients observed in THF/iodobenzene and CH_2Cl_2/iodobenzene are different states, more experiments (especially at times >5 ns) are necessary to prove this.

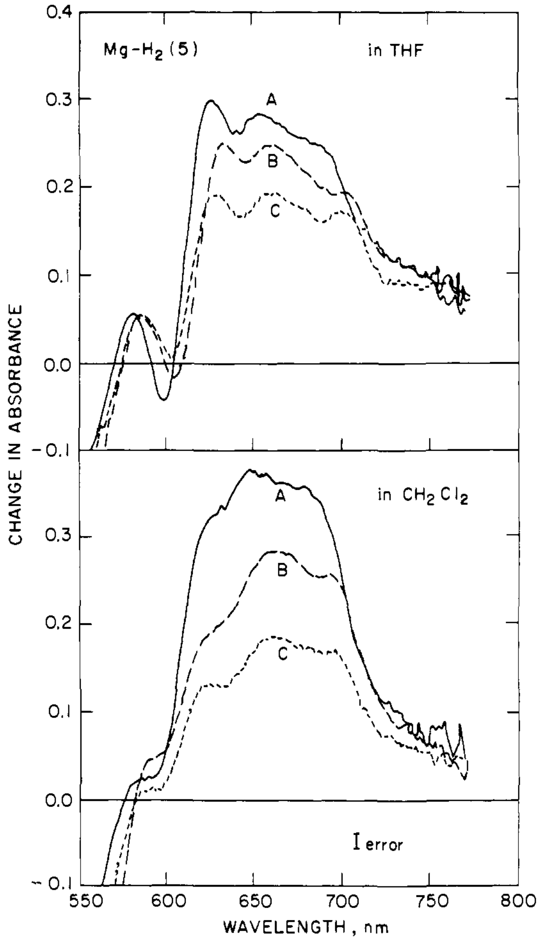

Figure 5. Change-in-absorbance spectra for 1.9 × 10^{-4} M Mg–H_2(5) in two solvents at t = 0 ps. For each solvent three concentrations of added p-benzoquinone were studied: A, 0.0 M; B, 0.25 M; and C, 0.50 M.

***p*-Benzoquinone Quenching in THF.** The general conclusion of studies of the quenching of the $^1(\pi,\pi^*)$ states of porphyrins and chlorophylls by quinones is that the quenching reaction returns the excited molecule to the ground state with very high efficiency (>0.95). However, recent work[16] has shown that when sufficient (>0.2 M) p-benzoquinone (BQ) is added to *meso*-tetraphenylporphine (TPP) to form ground state pairs between TPP and BQ, high yields (Y) of triplet states ($Y \geq 0.5$) can be achieved. The high triplet yields are possible, even with low quantum yields (Φ_T) for triplet formation ($\Phi_T < 0.05$), because of the extremely short S_1 state lifetime of the paired TPP molecules (0.3 ps < τ < 3 ps). Thus paired TPP molecules can be excited many times during a 6 ps (fwhm) photolysis pulse. As a first approximation, it is reasonable to expect BQ quenching of the S_1 state of Mg–H_2(5) to follow a similar pattern.

Curves A, B, and C in Figure 5 show the effects on the ΔA spectrum at 0 ps of adding respectively 0.0, 0.25, and 0.50 M BQ to Mg–H_2(5). The addition of BQ in both THF (top panel) and CH_2Cl_2 (bottom panel) decreases the observed ΔA signal. This is not due to absorption of the photolysis light by BQ, because even with 0.5 M BQ less than 10% of the 527-nm light is absorbed by BQ. Rather, this is evidence of ≪6 ps deactivation of some of the excited states through static quenching. Indeed, for 0.5

---

(16) Bergkamp, M. A.; Dalton, J.; Netzel, T. L. *J. Am. Chem. Soc.* **1982**, *104*, 253.

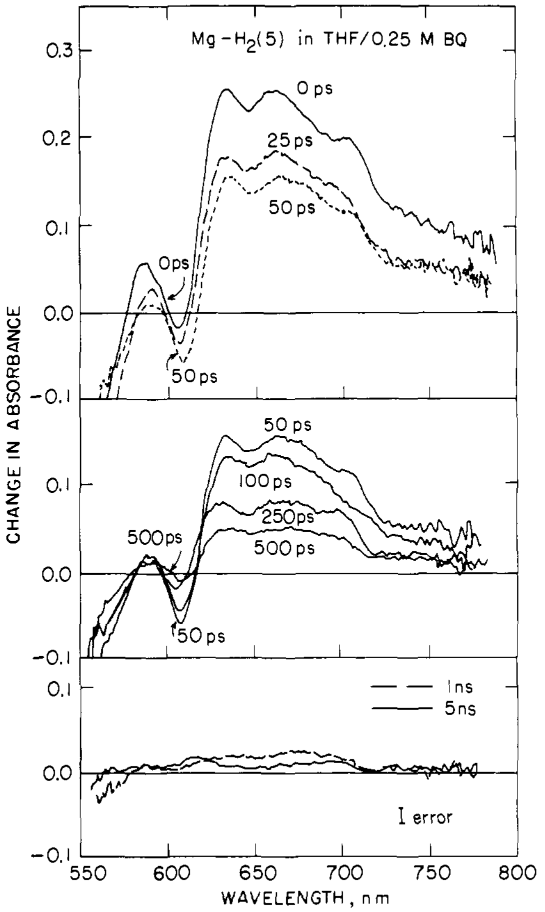

Figure 6. Change-in-absorbance spectra for 2.2 × 10^{-4} M Mg-H_2(5) in THF with 0.25 M *p*-benzoquinone added. The times after excitation are indicated. See Figure 7 for kinetic plots of these data.

M BQ additions, ΔA spectra taken during photolysis (−8 ps to 0 ps) show a transient of <6 ps duration. While the occurrence of static quenching in both THF and CH_2Cl_2 should be noted, the important observations concern the kinetic processes due to dynamic quenching in the two solvents.

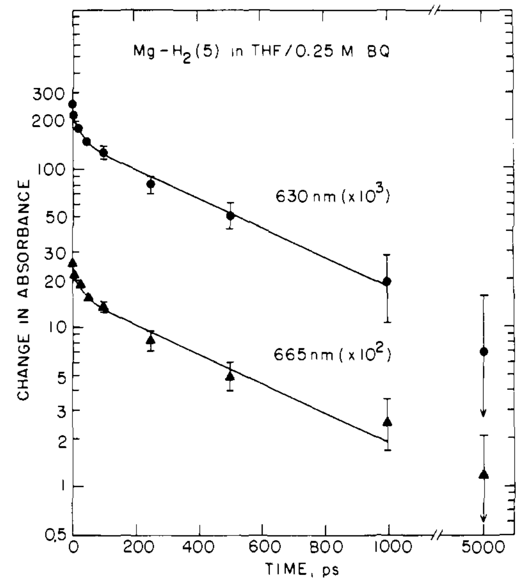

Figure 7. Kinetic plots of the ΔA data shown in Figure 6 at two wavelengths. The solid lines are calculated results based on eq 1 with the rate constants specified in Table I.

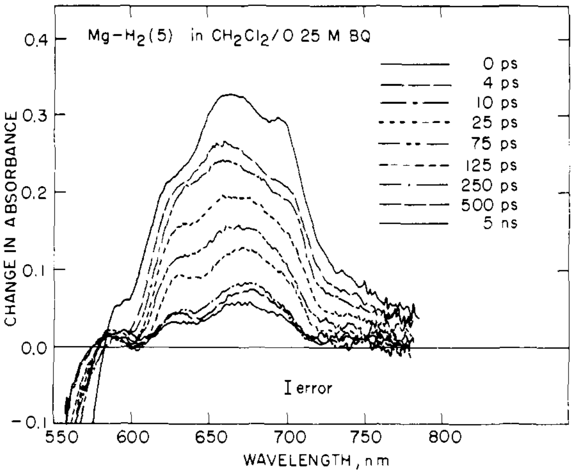

Figure 8. Change-in-absorbance spectra for 2.2 × 10^{-4} M Mg-H_2(5) in CH_2Cl_2 with 0.25 M *p*-benzoquinone added. The times after excitation are indicated. See Figure 9 for kinetic plots of these data.

Kinetic spectra for the quenching of Mg-H_2(5) by 0.25 M BQ in THF are shown in Figure 6 and plots of these data versus time at two wavelengths are shown in Figure 7. Two spectral results are worth emphasizing. First, a growth of ground state bleaching at 608 nm until 50 ps after photolysis shows that at least two excited states are kinetically important. This behavior has been reproduced in a 25% more concentrated sample with a corresponding increase in the amount of bleaching at 608 nm. Second, the ΔA spectrum taken 5 ns after excitation is zero within our error limits. This means that less than 2% of the sample is converted to a photoproduct with a molar absorptivity (ϵ) of 1 × 10^4 M^{-1} cm^{-1} in the 650-nm region (a typical value of molar absorptivity for porphyrin cations in the 600–700-nm region[17]). The kinetic analyses at 630 nm and 665 nm also indicate two distinct deactivation processes with lifetimes of 25 and 500 ps (see Table I). The most straightforward interpretation of these lifetimes is that the first corresponds to S_1 quenching and the second T_1 quenching. The appreciable yield of T_1 states could result from static quenching during the time of photolysis (vide supra) or from dynamic quenching of the S_1 states. However, it is unusual for dynamic quenching of the singlet states of monomeric prophyrins to yield large amounts of triplet states.[7,8] For comparison it is worth noting that a sample of TPP (6 × 10^{-4} M) in CH_2Cl_2 with 0.3 M BQ exhibited the following quenching dynamics:[16] (a) very rapid quenching (τ < 6 ps) of some of the S_1 states, (b) a slower S_1 state quenching (τ = 20 ± 10 ps), and (c) T_1 state quenching (τ = 860 ± 30 ps). The rates of S_1 and T_1 deactivation for TPP by BQ are therefore similar to the rates observed for the quenching of the excited states of Mg-H_2(5) by BQ. Similarly, the quantum yield of the long-lived (τ > 5 ns) tetraphenylporphine cation ($TPP^{+}\cdot$) was much less than 5%.

***p*-Benzoquinone Quenching in CH_2Cl_2.** Kinetic spectra for the quenching of Mg-H_2(5) in CH_2Cl_2 with 0.25 M BQ are shown in Figure 8. There is an abrupt spectral change between 0 ps and 4 ps. This could reflect either the end of the static quenching process with τ < 6 ps or a medium reorganization about the newly formed photoproduct. The kinetic data between 4 ps and 5 ns are plotted in Figure 9 at 635 and 665 nm. Two deactivation times are seen: 90 ± 5 ps and >15 ns (see Table I). Neither of these times is similar to the times found for BQ quenching of Mg-H_2(5) in THF or TPP in CH_2Cl_2. One of the most striking results is that an easily detectable amount of a long-lived (τ > 15 ns) photoproduct is formed. This photoproduct cannot be a singlet or triplet (π,π^*) state of the diporphyrin because it reacts too slowly with BQ. The most reasonable assignment of this state is $Mg^{+}\cdot$-H_2(5) + $BQ^{-}\cdot$. A lifetime of >50 ns is expected for these ions because they are both present at less than millimolar concentrations and cannot recombine at a faster than diffusion-controlled rate. While the spectrum of $Mg^{+}\cdot$-H_2(5) is currently unobtainable due to the instability of the oxidized diporphyrin, the spectrum of (magnesium octaethylporphine)$^{+}\cdot$ ($MgOEP^{+}\cdot$)

---

[17] Borg, D. C.; Fajer, J.; Felton, R. H. *Ann. N.Y. Acad. Sci.* **1973**, *206*, 177.

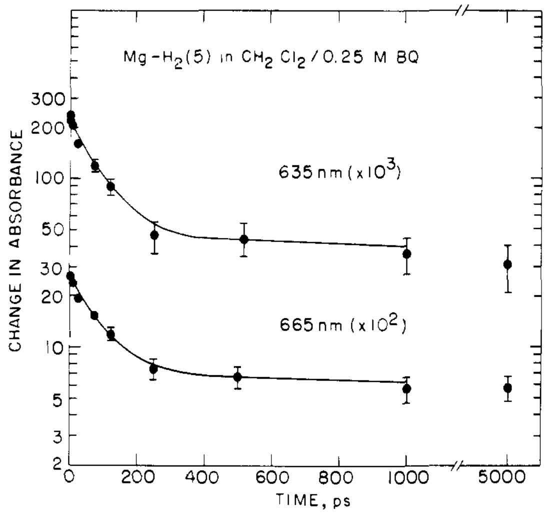

Figure 9. Kinetic plots of the ΔA data shown in Figure 8 at two wavelengths. The solid lines are calculated results based on eq 1 with the rate constants specified in Table I.

is known to have an absorption maximum at ~660 nm with ϵ of 1.2×10^4 M^{-1} cm^{-1}.[14,18] If $Mg^{+}\cdot{-}H_2(5)$ has this molar absorptivity at ~675 nm, its yield is ~12%. ($BQ^{-}\cdot$ does not absorb beyond 500 nm.[19]) The spectrum of $Mg^{+}\cdot{-}H_2^{-}\cdot(5)$ is likely to have increased absorption at 630 and 690 nm (on either side of the 660 nm (magnesium porphyrin)$^{+}\cdot$ peak) relative to that of $Mg^{+}\cdot{-}H_2(5)$ as well as an absorption band at 820 nm ($\epsilon \sim 8 \times 10^3$ M^{-1} cm^{-1}).[14,18] Unfortunately our SIT-vidicon detector is not sensitive beyond 775 nm. Thus the chief difference between the spectrum of $Mg^{+}\cdot{-}H_2^{-}\cdot(5)$ and $Mg^{+}\cdot{-}H_2(5)$ in the range 600–775 nm is likely to be that the former has a higher molar absorptivity and is somewhat broader than the latter. This description is consistent with assigning the 0 ps spectrum in Figure 8 to $Mg^{+}\cdot{-}H_2^{-}\cdot(5)$ and the spectra from 250 ps to 5 ns to $Mg^{+}\cdot{-}H_2(5)$. Note that we do not known the quantum yield of either species, so their molar absorptivities cannot be compared.

Only ~60% of the $Mg^{+}\cdot{-}H_2^{-}\cdot(5)$ formed in neat CH_2Cl_2 is present 4 ps after excitation in CH_2Cl_2 with 0.25 M BQ and its lifetime is reduced to 90 ps from 200 ps in neat CH_2Cl_2. If each quenching encounter produced $Mg^{+}\cdot{-}H_2(5)$, we would expect ~33% yield of this species. The ~12% yield observed implies that ~$^2/_3$ of the quenching encounters "short-circuit" $Mg^{+}\cdot{-}H_2^{-}\cdot(5)$ and re-form the starting material. Presumably these "short-circuiting" reactions represent encounters near the interface of the porphyrin subunits.

It is interesting to compare the 250-ps spectrum of Figure 8 and the 5-ns spectrum of Figure 4. The two are similar with the latter being somewhat broader than the former. This is how the ΔA spectra for $Mg^{+}\cdot{-}H_2(5)$ would be expected to differ from that of $Mg^{+}\cdot{-}H_2^{-}\cdot(5)$ and suggest that the 5-ns spectrum in Figure 4 could be a $^3(Mg^{+}\cdot{-}H_2^{-}\cdot)$ species. Kinetic studies beyond 5 ns are necessary to determine whether or not this is actually the case.

Discussion and Conclusion

Time-resolved excited-state absorption spectra of $Mg{-}H_2(5)$ in THF and in THF/iodobenzene (1:1) show an increase in the intersystem crossing rate ($S_1 \rightarrow T_1$) in the later solvent (S_1 lifetime reduced to 650 ps from ~2 ns). By way of comparison, the short time (τ = 200 ps) decay kinetics of photoexcited $Mg{-}H_2(5)$ in CH_2Cl_2 are unaffected by changing to CH_2Cl_2/iodobenzene as the solvent and the lifetime of the second transient may be increased slightly (from ~6 ns to ~13 ns) upon the addition of iodobenzene. But even this longer lifetime (~13 ns) in CH_2Cl_2/iodobenzene is inconsistent with it being a $^3(\pi,\pi^*)$ state, as these states in magnesium and free-base porphyrins do not decay in <50 ns.[20] The BQ quenching of the $Mg{-}H_2(5)$ excited states in THF showed two distinct relaxation processes, similar to the S_1 and T_1 quenching reaction observed for TPP.[16] The T_1 state lifetime was ~0.5 ns and less than 2% of a $Mg^{+}\cdot{-}H_2$ species was present 5 ns after excitation. In contrast, BQ quenching of $Mg{-}H_2(5)$ in CH_2Cl_2 produced an easily observable photoproduct with a lifetime >15 ns. The quenching reaction to form this species shortened the primary photoproduct's lifetime to 90 ps. The most reasonable assignment of the second species is $Mg^{+}\cdot{-}H_2 + BQ^{-}\cdot$. Comparison of its spectrum with that of $MgOEP^{+}\cdot$ suggests that its yield is ~12%. The differences in the above kinetic processes for $Mg{-}H_2(5)$ in CH_2Cl_2 and THF are easily explained if the first observed photoproduct is $Mg^{+}\cdot{-}H_2^{-}\cdot$ in CH_2Cl_2 and a (π,π^*) singlet state in THF. It is difficult to ascribe these differences to solvent perturbations of a single type of excited state.

The nature of the second state formed by the decay of $^1[Mg^{+}\cdot{-}H_2^{-}\cdot]$ in CH_2Cl_2 is an open question. The fact that its difference spectrum is similar to that of $Mg^{+}\cdot{-}H_2$ and not to that of the T_1 state of $Mg{-}H_2(5)$ suggests that it may be a triplet biradical, $^3[Mg^{+}\cdot{-}H_2^{-}\cdot]$. That it decays in the 5–15 ns time domain supports this suggestion.

The important result of these studies is the confirmation of the previous[6] assignment of a rapid (<6 ps) electron transfer after photoexciting $Mg{-}H_2(5)$ in CH_2Cl_2. In view of this, it is worth suggesting a model to account for the rapid $S_1 \rightarrow$ ET reaction ($k > 2 \times 10^{11}$ s^{-1}) and slow reverse ET ($k = 5 \times 10^9$ s^{-1}) to re-form the ground state. The specific point that we wish to address is the slow rate of the reverse ET. Therefore the small portion of the initial ET product, $^1[Mg^{+}\cdot{-}H_2^{-}\cdot]$, which decays to another state [perhaps $^3(Mg^{+}\cdot{-}H_2^{-}\cdot)$] will be neglected in the following discussion. Presumably the lifetime of $^1[Mg^{+}\cdot{-}H_2^{-}\cdot]$ would be even longer than 200 ps if its only decay route were reverse ET to S_0. The novelty of this result for in vitro systems (although expected on the basis of in vivo studies on photosynthetic systems) can be emphasized by noting that previous attempts[7,8] to quench the singlet states of porphyrins and chlorophylls with quinones and nitroaromatics failed to produce detectable ET photoproducts. Indeed, study of *meso*-triphenyl(*p*-benzoquinone)porphine[16] showed that while its S_1 state was shortened to <6 ps, only T_1 and not ET products were produced by S_1 quenching.

The rapid rate of ET in the forward direction, to form $Mg^{+}\cdot{-}H_2^{-}\cdot$, demonstrates that the electronic coupling, V, for this process is large. There is no reason to assume that it is significantly smaller for the reverse ET, yet that process is much slower. What is the nature of the barrier which slows the reverse reaction? Resonance Raman data on porphyrins and their ions[21] show that they have similar vibrational frequencies. Also, the X-ray crystal structure of the zinc tetraphenylporphine cation[22] shows that its bond distances and angles are similar to those of other metalloporphyrins. These facts suggest that the energy requirements for internal nuclear reorganization accompanying ET in either direction for $Mg{-}H_2(5)$ are small.[23,24] Similarly, the large size of the diporphyrin implies that the solvent reorganization energy will not be large.[23,24] Consequently the minium of the potential energy surface for $Mg^{+}\cdot{-}H_2^{-}\cdot$ is probably only slightly displaced relative to the minima of the S_1 and ground states of $Mg{-}H_2(5)$ (Δ_f and Δ_r, respectively).

If a critical nuclear displacement coordinate or an effective displacement coordinate can be defined such that motions along it govern the observed ET reactions, only this dimension of the relevant potential energy surfaces need be explicitly discussed.[25-27]

---

[18] Netzel, T. L. In "Primary events in Biology Probed by Ultrafast Laser Spectroscopy", R. R. Alfano, Ed., Academic Press: New York, in press.

[19] Bridge, N. K.; Porter, G. *R. Soc. London, Ser. A* **1958**, *244*, 259; **1958**, *244*, 276.

[20] Gradzushko, A. T.; Mashenkov, V. A.; Sevchenko, A. N.; Solov'ev, K. N.; Tsvirko, M. P. *Sov. Phys. Dokl.* (*Engl. Transl.*) **1969**, *13*, 869.

[21] Felton, R. H.; Yu, N. T. In "Porphyrins", D. Dolphin, Ed.; Academic Press, New York, 1978; Vol. III, p 347.

[22] Spaulding, L. D.; Eller, P. G.; Bertrand, J. A.; Felton, R. H. *J. Am. Chem. Soc.* **1974**, *96*, 982.

[23] Sutin, N. *Annu. Rev. Nucl. Sci.* **1962**, *12*, 285.

[24] Marcus, R. A. *Annu. rev. Phys. Chem.* **1964**, *15*, 155.

[25] Reynolds, W. L.; Lumry, R. W. In "Mechanisms of Electron Transfer"; Ronald Press: New York, 1966.

[26] Levich, V. G. *Adv. Electrochem. Eng.* **1966**, *4*, 249.

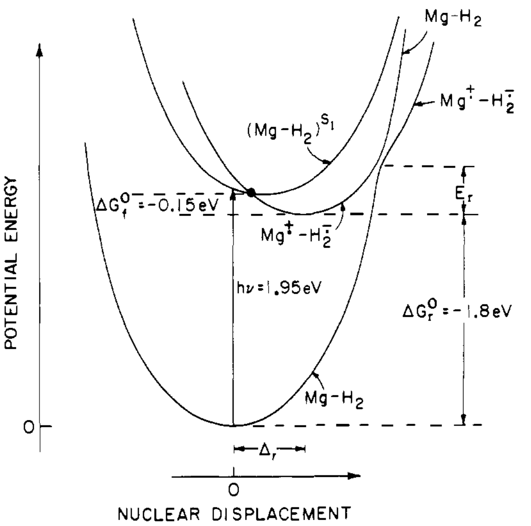

Figure 10. Potential energy vs. nuclear displacement curves for the ground state of Mg–H_2(5), (Mg–H_2)^{S_1}, and $Mg^{+}\cdot$–$H_2^{-}\cdot$. $\Delta G_f°$ and $\Delta G_r°$ are, respectively, the differences in free energy in CH_2Cl_2 for the (Mg–H_2)^{S_1} → $Mg^{+}\cdot$–$H_2^{-}\cdot$ and $Mg^{+}\cdot$–$H_2^{-}\cdot$ → Mg–H_2 reactions. E_r is the energy of the avoided crossing region above the minimum of the $Mg^{+}\cdot$–$H_2^{-}\cdot$ curve. Δ_r is the nuclear displacement between the minima of the $Mg^{+}\cdot$–$H_2^{-}\cdot$ and Mg–H_2 curves.

One objective of work on unimolecular complexes such as Mg–H_2(5) is to assess the appropriateness of this approximation. With this in mind, we can discuss the ET paths for Mg–H_2(5) in terms of the potential curves shown in Figure 10. The free-energy difference, $\Delta G_r°$, was obtained from previously reported[6] electrochemical measurements for Mg–H_2(5) in CH_2Cl_2. Note that the energy of the S_1 state is an enthalpy change. Comparing this quantity to $\Delta G_r°$ is appropriate only if the entropy changes associated with excited state formation are small.

The curves in Figure 10 show that the reverse ET is nonadiabatic due to an avoided crossing at height E_r above the minium of the $Mg^{+}\cdot$–$H_2^{-}\cdot$ potential energy curve. For this type of ET, the rate is governed by both an electronic factor reflecting the nonadiabatic character of the ET and Franck–Condon overlap integrals which determine the frequency of nuclear tunneling from the reactant potential energy surface to that of the product.[27,28] This kinetic bottleneck is caused by both a large $\Delta G_r°$, ca. −1.8 eV, and weak electron-vibration coupling (a small Δ_r). By contrast, the forward ET

$$(\mathrm{Mg{-}H_2})^{S_1} \xrightarrow{>10^{11}\ \mathrm{s}^{-1}} \mathrm{Mg}^{+}\cdot{-}\mathrm{H_2}^{-}\cdot$$

is likely to be nearly activationless, because although the displacement between the two potential energy curves (Δ_f) is small, $\Delta G_f°$ is also small. Jortner[29] has recently emphasized the following characteristics of an activationless ET: (1) the low-temperature rate "essentially provides a determination of the electronic coupling V", and (2) at high temperatures there is an apparent negative activation energy because the ET rate is proportional to $(1/T)^{1/2}$.

If the reverse ET is governed by the location of an avoided crossing between two steeply rising functions, it may be sensitive to changes of solvent or altered diporphyrin geometries. At the same time, changes in $\Delta G_f°$ or in the amount of nuclear displacement (Δ_f) are less likely to affect the forward ET, since the curves for the S_1 and $Mg^{+}\cdot$–$H_2^{-}\cdot$ states cross near the minimum of the S_1 potential energy function. Whether increasing the solvent reorganization energy can dominate electronic factors and Franck–Condon overlap integrals and speed up the reverse ET is difficult to predict in advance of the experiment. Current work is examining the effects of variations in solvent and diporphyrin structure on the forward and reverse ET processes.

It is interesting to compare the properties of the Mg–H_2(5) diporphyrin in CH_2Cl_2 to those of the electron donor–acceptor components in reaction centers of photosynthetic bacteria. In *Rps. Sphaeroides* RCs, the oxidation of the primary electron donor, $(BChl)_2$, proceeds at a rate $>10^{11}$ s^{-1}.[4,5,30] In Mg–H_2(5), the rate of the S_1 → ET reaction is similarly fast, $>10^{11}$ s^{-1}. In RCs the apparent difference in energy between the S_1 state of the electron donor and the free energy of formation of the ET product, $(BChl)_2^{+}\cdot BPheo^{-}\cdot$, is 50–130 meV[18,31,32] vs. 150 meV for Mg–H_2(5).[6] Consequently, both this diporphyrin and bacterial RCs store >90% of the incident photon's energy in their ET products. A recent estimate[33] of the edge-to-edge distance of the primary charge separation to form $(BChl)_2^{+}\cdot BChl^{-}\cdot$ [a possible precursor of $(BChl)_2^{+}\cdot BPheo^{-}\cdot$] is ~3.1 Å. In contrast, the edges of the porphyrin subunits in Mg–H_2(5) are less than 1 Å apart.[13] Finally, although the primary electron donor in purple photosynthetic bacteria is a dimer, work on Mg–H_2(5) shows that a dimeric electron donor is not obligatory. Indeed, Mg–H_2(5) is a good model of the primary electron donor–acceptor pair of PSII in green plants. In this case a ligated chlorophyll monomer is the postulated electron donor[34] and pheophytin the acceptor.[3,35]

Acknowledgment. This work was supported by the Office of Basic Energy Sciences of the U.S. Department of Energy at Brookhaven National Laboratory and by the Research Corporation and the National Science Foundation at M.S.U.

We thank Dr. N. Sutin for his helpful comments concerning this manuscript and Drs. J. Fajer and I. Fujita for many helpful discussions.

Registry No. Mg-H_2(5), 73817-06-8.

---

(27) Brunschwig, B. S.; Logan, J.; Newton, M.; Sutin, N. *J. Am. Chem. Soc.* **1980**, *102*, 5798.

(28) Jortner, J. *J. Chem. Phys.* **1976**, *64*, 4860.

(29) Jortner, J. *J. Am. Chem. Soc.* **1980**, *102*, 6676.

(30) Holten, D.; Hoganson, C.; Windsor, W. M.; Schneck, C. C.; Parson, W. W.; Migus, A.; Fork, R. L.; Shank, C. U. *Biochim. Biophys. Acta* **1980**, *592*, 461.

(31) van Grondelle, R.; Holmes, N. G.; Rademaker, H.; Duysens, L. N. M. *Biochim. Biophys. Acta* **1978**, *253*, 187.

(32) Klimov, V. V.; Shuvalov, V. A.; Krakhmaleva, I. N.; Klevanik, A. V.; Krasnovsky, A. A. *Biokhimiya (Moscow)* **1977**, *42*, 519.

(33) Shuvalov, V. A.; Parson, W. W. *Proc. Natl. Acad. Sci. U.S.A.* **1981**, *78*, 957.

(34) Davis, M. S.; Forman, A.; Fajer, J. *Proc. Natl. Acad. Sci. U.S.A.* **1979**, *76*, 4170.

(35) Fajer, J.; Davis, M. S.; Forman, A.; Klimov, V. V.; Dolan, E.; Ke, B. *J. Am. Chem. Soc.* **1980**, *102*, 7143.